RSC Advances

ROYAL SOCIETY OF CHEMISTRY

www.rsc.org/advances

Cite this: DOI: 10.1039/c0xx00000x

www.rsc.org/xxxxxx

Paper

Controllable and Mass Fabrication of Highly Luminescent N-doped Carbon Dots for Bioimaging Applications

Zhao Chen,[a,b] Xiaochi Wang,[a] Hua Li,[c] Chao Li,[d] Qinghua Lu,[b] Guang Yang,[d] Jiangang Long,[c] and Lingjie Meng*[a]

Received (in XXX, XXX) Xth XXXXXXXXX 20XX, Accepted Xth XXXXXXXXX 20XX
DOI: 10.1039/b000000x

Abstract: A facile but effective bottom-up method for the mass preparation of N-doped carbon dots (N-C-dots) was developed by the direct heating of a solid mixture of folic acid (FA) and sodium citrate (SC) for several minutes at 300 °C. The nitrogen content of the resulting N-C-dots could be easily and precisely tuned from 0% to 14% by adjusting the SC to FA mass ratio. Uniform N-C-dots with honeycomb-like ordered structures were obtained, with sizes ranging from 1 to 3 nm in diameter. The N-doping content affected not only the emission quantum yield but also the emission wavelength. The N-C-dots emitted strong blue–green fluorescence based on the excitation wavelength and N-doping content. Because of their excellent water solubility, low toxicity, powerful fluorescence, and high resistance to photobleaching, the N-C-dots can enter various cells and serve as ideal candidates for multicolour cell imaging.

1. Introduction

Carbon dots (C-dots) represent a fascinating class of emerging carbon nanomaterials owing to their unique properties such as tunable luminescence, superior chemical and fluorescence stability, excellent biocompatibility, and versatile surface chemistry.[1-6] The optical properties of C-dots can be regulated by their sizes, surfaces, and edges.[7-9] For example, by surface passivation with different organic moieties,[10-12] C-dots could emit fluorescence ranging from blue to near infrared region. Other than morphology and surface control, chemical doping is a newfound strategy to adjust the photoluminescence (PL) wavelength and improve the quantum yield (QY) of C-dots as well. In particular, the N-doped C-dots (N-C-dots) have attracted significant attention in recent three years for improving fluorescence performance and broadening their applications.[13-21]

For these reasons, it is imperative to develop effective methods for preparing C-dots and N-C-dots for various applications. Two basic strategies have been proposed: "top-down" methods by cutting the carbon resources[22-27] and "bottom-up" approaches by chemical synthesis from small organic molecules.[28-39] N-C-dots were typically synthesized by the "bottom-up" strategy, which involved carbonizing the mixtures of N-sources (urea,[14] ammonia,[15] hydroxylamine,[30] amoxicillin,[31] NaNH,[32] dimethylamine,[33] among others) and C-sources under hydrothermal or microwave-assisted hydrothermal conditions. However, these fabrication methods were often time-consuming; they also afforded low yield of products and were difficult to extend to mass production and to precisely control the N-doping content.

Herein, we developed a facile but effective synthesis to prepare N-C-dots in one-pot by directly heating a solid mixture of folic acid (FA) and sodium citrate (SC) for several minutes. The N-doping content of the resulting N-C-dots could be well tuned from 0% to 14% by adjusting the mass ratio of SC to FA. Through systematic investigations, we found that the N-doping content affected not only the QY but also the emission wavelength. This method provides a new method for the mass production (several grams or more) of N-C-dots with tunable emissions for various applications. Owing to their good water solubility, low toxicity, and strong fluorescence, the N-C-dots

were directly applied in cell imaging to demonstrate one of their promising applications.

2. Experimental

2.1. Materials

Sodium citrate (SC, 99%) and folic acid (FA, 97%) were purchased from Aladdin Reagent Corporation. The human cervical cell line HeLa and rat cardiomyoblast cell line H9C2 were purchased from the Cell Resource Centre of Life Sciences in Shanghai. The porous poly(vinylidene chloride) (PVDC) membrane was purchased from the Shanghai ANPEL Instrument Co., Ltd. (50 mm diameter and 0.22 μm pore size). Bovine serum albumin (BSA) were obtained from Shanghai Chemical Reagent Corporation. Fetal bovine serum (FBS) and high-glucose Dulbecco's modified Eagle's medium (DMEM) were obtained from Hyclone. MTT reagent was purchased from Beyondtime Bio-Tech, China. Other chemicals were analytically pure and used as received. Water was purified using a Milli-Q-system (Millipore, Bedford).

2.2. Characterization: High resolution-transmission electron microscopy (HRTEM) was conducted on a JEOL JEM-ARM200 operates at 200 kV. The sizes and distribution of all as-prepared nanomaterials were determined from TEM micrographs using ImageJ (V1.41, NIH, USA) for image analysis. X-ray photoelectron spectroscopy (XPS) experiments were carried out on an AXIS ULtrabld system (Kratos) with Mg Kα radiation (hν= 1253.6 eV) or Al Kα radiation (hν = 1486.6 eV). The Fourier transform infrared (FTIR) spectra were obtained on a FTIR spectrophotometer (Thermo Nicolet 360). UV–Vis absorption was characterized by a UV-Vis-NIR spectrophotometer (Lambda 750). Zeta potentials were measured on a zeta potential analyzer (Zetasizer Nano ZS90, Malvern). All fluorescence spectra, absolute quantum yield and fluorescence lifetimes were measured with a FLS920 lifetime and steady state spectrometer with a calibrated integrating sphere (Edinburgh). Raman spectra were registered with a HR800 Raman spectrometer (Horiba) at 514 nm on a copper foil. Fluorescence images of cells were taken on a LSM700 confocal laser scanning microscopy (Carl Zeiss).

2.3 Synthesis of C-dots and N-C-dots: In a typical procedure, the mixture of SC and FA (2.0 g) at different mass ratio (1:0, 40:1, 20:1, 10:1, 6.7:1, 5:1, 2.5:1, 2:1, 1:1, 1:2, 1:4, and 0:1) was fully grinded in an agate mortar. The mixed powders were placed into glass tubes and heated at 300 °C in an oil bath for 4 min. The resulting black or brown solid was dissolved in pure water (10 mL) and filtered through a PVDF membrane, resulting the C-dot or N-C-dot aqueous solution.

2.4 Cell viability test: The MTT assay was used to measure cell viability.[34-35] In brief, HeLa cells and H9C2 cells were seeded into a 96-well flat culture plate (Corning) and cultured in DMEM supplemented with 10% FBS, 100 units/mL penicillin and 100 μg/mL streptomycin, at 37 °C in a humidified incubator (MCO-15AC, Sanyo) in which the CO_2 level was kept constant at 5%. After culturing overnight, the cells were washed with FBS-free DMEM and incubated with a specific concentration of N-C-dots (10, 25, 50, 100 μg/mL) in FBS-free culture medium at 37 °C for 24 and 48 h, respectively. The cells were then washed with PBS, and FBS-free DMEM (100 μL) was used to substitute the culture medium before adding 1/10 (V/V) of MTT reagent. After incubation for another 3 h at 37 °C, the medium was removed and 200 μL DMSO was added into each well to dissolve the formazan. And the absorbance was measured at 470 nm using a microplate reader (Model 680, Bio-Rad) after shaking 15 min. The background absorbance was measured at 470 nm before adding the MTT reagent and the cells cultured in the absence of N-C-dots were used as controls.

2.5 Cell imaging by confocal laser scanning microscopy: The cell imaging capacity of the N-C-dots was investigated by means of confocal laser scanning microscopy. HeLa cells and H9C2 cells were seeded into a 24-well flat culture plate (Corning) and cultured in DMEM supplemented with 10% FBS, 100 units/mL penicillin and 100 μg/mL streptomycin at 37 °C overnight. The cells were washed with FBS-free DMEM and incubated with N-C-dots (50 μg/mL) in FBS-free culture medium at 37 °C for another 4 h. The cells were then washed with PBS and FBS-free DMEM to remove the free N-C-dots from the culture medium.

The cells were then observed under a confocal laser scanning microscopy.

3. Results and Discussion

3.1. Preparation and morphology of N-C-dots

N-C-dots were prepared by a very simple one-pot reaction of SC and FA by thermopolymerization and dehydrogenation for several minutes (Scheme 1). After the mixed powder of SC and FA was placed in an oil bath at 300 °C, the powder began to melt within 30 s and was almost fully converted to a liquid within 3.5 min. The colour of the liquid gradually changed to brown and black, indicating that C-dots or N-C-dots are formed. The resulting products were taken out and allowed to cool to ambient temperature.

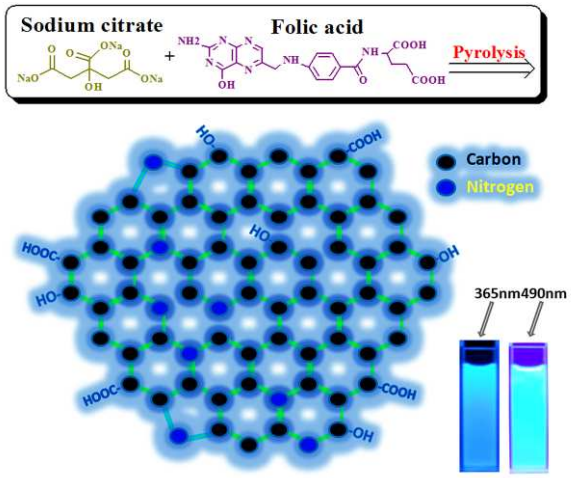

Scheme 1. Schematic of the synthetic route to N-C-dots

The PL property of N-C-dots is closely related to their concentration and the degree of thermopolymerization; thus, the reaction time and concentration were optimized through fluorescence tests. An aqueous N-C-dot solution emitted a bright fluorescence under light irradiation of 365 nm. The fluorescence intensity increased with increasing N-C-dot concentration and reached a maximum at about 0.5 mg/mL (see Supporting Information, Figure S1). With further increase in the N-C-dot concentration, the fluorescence intensity decreased, probably because of the aggregation of the N-C-dots, thereby resulting in fluorescence quenching. Based on the result, we further investigated the fluorescence intensity of 0.5 mg/mL N-C-dots prepared at different reaction times. The N-C-dots prepared at 300 °C for 4 min exhibited the strongest fluorescence (see Supporting Information, Figure S2), suggesting that the optimal reaction time is approximately 4 min.

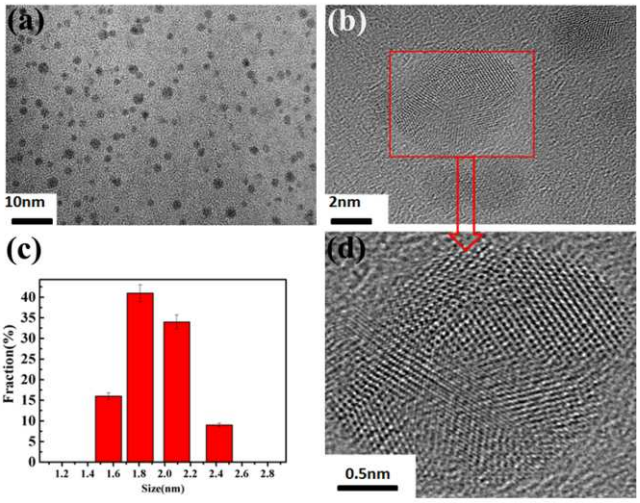

Figure 1. (a,b) HRTEM images of N-C-dots (SC to FA mass ratio is 20:1). (c) Size distribution of N-C-dots in (a). (d) amplified HRTEM of N-C-dots in (b).

The sizes and structures of the as-synthesized N-C-dots were investigated by HRTEM. Figure 1 shows typical HRTEM images of N-C-dots derived from an SC:FA mixture of 20:1. As shown in Figures 1a and 1c, relatively uniform N-C-dots were observed, with sizes ranging from 1 to 3 nm in diameter. The magnified image provides direct evidence that SC and FA react with each other to form N-C-dots with clear lattice fringes, which is similar to those reported previously.[23,36] Along with amorphous ultrathin carbon-coated structures on TEM grids, honeycomb-like structures were observed in some regions of the N-C-dots, with each honeycomb-like hole being approximately 0.12 nm (Figure 1d). The partially ordered structures in the dots might benefit the fluorescence property. All other samples exhibited size and morphology similar to those in Figure 1.

3.2 Structure characterization of N-C-dots

FTIR spectroscopy was used to compare the structures of C-dots and N-C-dots with those of their precursors (Figure 2a). Compared with the FTIR spectrum of SC, that of C-dots prepared from pure SC exhibited a new characteristic absorption peak at

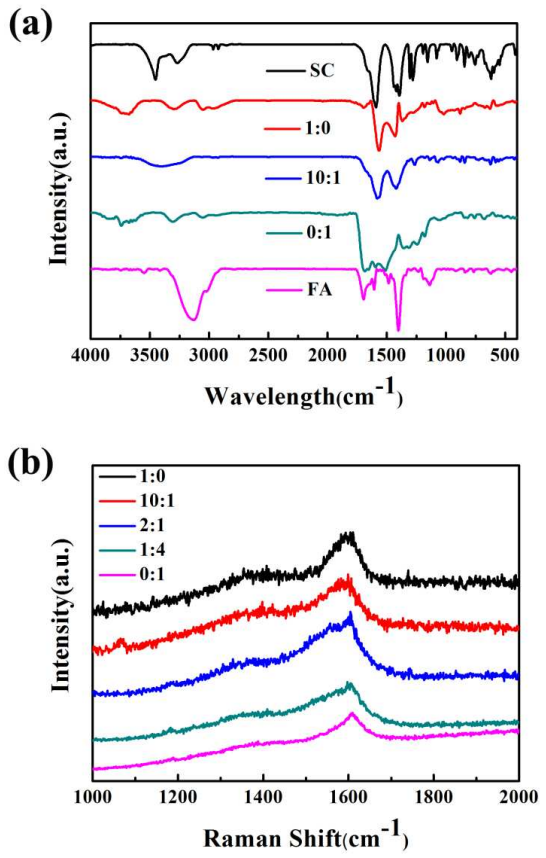

Figure 2. (a) FTIR spectra of the C-dots, N-C-dots and their raw materials. (b) Raman spectra of N-C-dots derived from different SC:FA mass ratios.

3060 cm^{-1}, indicating the formation of C=C bonds during the reaction. In the C-dot spectrum, the peaks at 1690, 2950, and 3300 cm^{-1} corresponded to the stretching vibrations of OH, CH_2, and C=O groups, respectively, implying that C-dots still contain some COOH and CH_2 groups and that carbonization is not complete. In the FTIR spectrum of N-C-dots prepared from pure FA, the peaks at 3200 and 1390 cm^{-1} corresponding to NH_2 and NH groups, respectively, almost disappeared, probably because amides react with neighboring carboxylic groups by intra- and intermolecular dehydrolysis. However, the peaks at 1690 and 3300 cm^{-1} corresponding to the stretching vibrations of OH and C=O groups, respectively, were still observed, implying that the N-C-dots also contain some COOH. Of note, the C=N vibration peak at 1670 cm^{-1} gradually increased proportionally with the FA content (see Supporting Information, Figure S3).

Raman spectra provided additional evidence that all the obtained C-dots and N-C-dots have ordered microstructures (Figure 2b). All samples exhibited an obvious peak at 1600 cm^{-1}, which is the characteristic tangential displacement mode of the highly crystalline graphite. In addition, the D band at approximately 1350 cm^{-1} resulting from amorphous carbon and defects weakened with increasing FA content, probably because the rigid pteridine rings of FA might aid in the formation of ordered structures in N-C-dots.

The actual N-doping content in the N-C-dots was studied by XPS analysis (Figure 3 and Table 1). In the XPS spectra of N-C-dot samples, the peaks at approximately 400 and 284 eV corresponded to N1s and C1s, respectively. The nitrous content of the C-dots was zero since the SC precursor did not contain any nitrogen element. Interestingly, the nitrous content in the N-C-dots increased proportionally to the FA:SC mass ratio. An increase of approximately 1.4% in the nitrous content for the N-C-dots corresponded to a 10% increase of FA in the precursor mixtures. Therefore, the N-doping content of the resulting C-dots can be tuned from 0% to 14% in a facile and quantitative manner by adjusting the SC:FA mass ratio. On the other hand, FA had a significantly lower content of C–O and C=O than SC. The oxygenated carbon decreased as a result of the increase of the FA:SC mass ratio. In addition, the Zeta potentials of the N-C-dots increased with increasing nitrous content (Table 1), which is in good agreement with the results obtained from XPS.

Table.1 Zeta potentials of C-dots and N-C-dots

Sample (SC:FA)	Zeta Potential[a] [mV]
1:0	-40.7
10:1	-37.5
2:1	-32.7
0:1	-18

[a] Values are averaged from three measurements.

XPS is a standard technique for studying the nitrogen and carbon configurations through N 1s and C 1s spectra.[37-38] In the C 1s spectra of N-C-dots, four peaks were deconvoluted: C=C peak

at 284.66 eV, C–C peak at 285.39 eV, C–O/C–N peak at 286.1 eV, and C=O/C=N peak at 287.59 eV (see Figure 3 and Supporting Information, Table S1). The C–C configuration constitutes the majority of carbon atoms in a C-dot sample, indicating that most of carbon atoms are sp^3 hybridized, and only small sp^2 clusters are isolated within the incompletely carbonized C-dots. With increasing FA:SC mass ratio, the content of C=C gradually increased because the pteridine and benzene rings of FA were maintained. In addition, three common bonding configurations may be obtained when doping nitrogen into the C-dots: pyridinic N (398.38 eV), pyrrolic N (399.08 eV), and quaternary N (400.14 eV). At a low FA:SC mass ratio, the amino and imino groups on FA were significantly lesser than the carboxyl groups on FA and SC; multiple carboxyl groups might react with one amino group and lead to high quaternary N content. With increasing FA:SC mass ratio, the amount of quaternary N gradually decreased, while that of pyridinic N increased correspondingly (see the inset in Figure 3 and Supporting Information, Table S1).

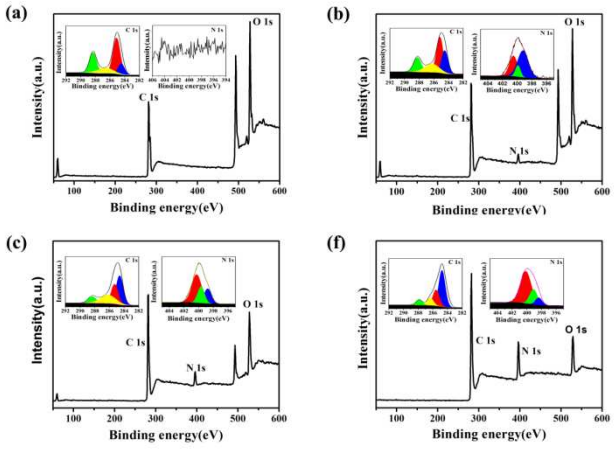

Figure 3. XPS full-scan survey. Inset: high-resolution C 1s and N 1s XPS spectra. The mass ratio of FA to SC is (a) 0:1, (b) 1:10, (c) 1:2, and (d) 1:0.

3.3 Optical properties of N-C-dots

The absorption properties of the as-prepared C-dots and N-C-dots were investigated by UV-Vis spectroscopy (Figure 4a). The aqueous solution of C-dots derived from pure SC exhibited no obvious absorbance peak between 250 and 600 nm, indicating the lack of large conjugate structures. Combining the results of HRTEM and XPS analysis, we concluded that the honeycomb-like structures of C-dots do not have any aromatic rings and only contain some C=C bonds. With increasing FA content, the aqueous solutions of N-C-dots gradually became darker and exhibited two dominant absorbance peaks at 270 and 365 nm, respectively. The absorption curves of N-C-dots were very similar to those of FA, except for slight peak broadening and a small blue shift, implying that the conjugated FA structure is mainly maintained during the reaction.

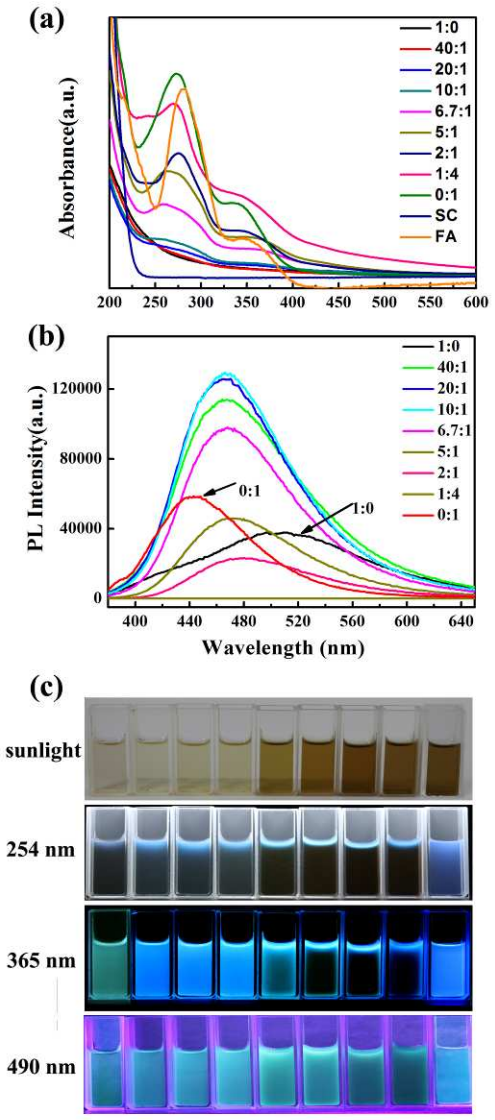

Figure 4. (a) UV-Vis spectra of the as-prepared C-dots, N-C-dots as well as SC and FA. (b) PL spectra of as-prepared C-dots and

N-C-dots dispersed in water under light irradiation of 365 nm. (c) Photographs of N-C-dot aqueous solution at 0.5 mg/mL under natural light excitation, 254, 365, and 490 nm light (SC to FA mass ratio increased from left to right).

Based on the UV-Vis spectra, the fluorescent properties of C-dots and N-C-dots were compared under light irradiation of 254, 365, and 490 nm (Figure 4c). All samples exhibited very weak or no PL under light excitation of 254 nm (Figure 4a and c); however, they emitted strong luminescence under light irradiation of 365 and 490 nm. The maximum emission wavelength of C-dots and N-C-dots derived from pure SC and FA was 520 and 445 nm under light irradiation of 365 nm, respectively, while that of all other N-C-dots was 475 nm (Figure 4b). Interestingly, all the samples emitted strong green fluorescence under exposure to 490 nm (Figure 4c), and their maximum emission wavelength was about 550 nm with a half-peak width of approximately 70 nm (see Supporting Information, Figure S4).

The exact fluorescence mechanism of C-dots and N-C-dots remains to be elucidated. We proposed that several sp^2 clusters were isolated within the sp^3 C–C, C–N, and C–O matrix to prevent the formation of large conjugated structures;[39-40] therefore, only blue and green fluorescence can be observed. It is consistent with the results of XPS and UV-Vis spectra. Interestingly, the fluorescence QY is closely related to the SC:FA mass ratio. For example, the QY of C-dots under light irradiation of 365 nm was approximately 1.3%, and the QY of N-C-dots reached 4.56% when the FA:SC mass ratio increased to 1:10. With further increase in the FA content, the QY and fluorescence intensity of N-C-dots gradually decreased, and the emission almost disappeared at a FA:SC mass ratio of 1:1 or greater. Remarkably, the QY of N-C-dots prepared from pure FA dramatically increased to 28.39%, probably caused by the involvement of a totally different reaction mechanism and formation of a new structure. Therefore, the N content affected not only the maximum emission wavelength but also the fluorescence QY. The substitution of N atoms, which introduces the unpaired electron, might change the atomic charge distribution and electronic gap. This can be indirectly demonstrated by the fluorescence lifetime. With increasing N-doping content, the lifetime gradually increased from 4.57 ns to 12.5 ns (see Supporting Information, Figure S5).

Photostability is a particularly important criterion in cases in which it is often desirable to observe markers for extended periods against the background of intrinsic cellular emissions. Remarkably, the N-C-dots were quite stable under light irradiation of 365 nm (2 W) and exhibited only negligible reduction in the observed intensities for 30 min (see Supporting Information, Figure S6).

3.4 Cell imaging applications

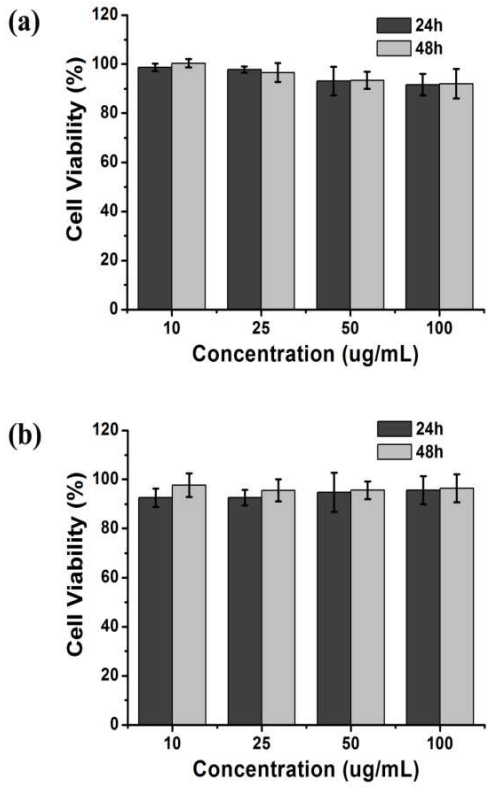

Figure 5. Viability of (a) HeLa and (b) H9C2 cells incubated with N-C-dots at diverse concentrations for 24 h (black) and 48 h (gray) determined by the MTT assay.

All biomaterials are expected to exhibit an intrinsically low toxicity; thus, the safety of N-C-dots is a primary concern for use in biomedical applications. The cytotoxicity of N-C-dots was

quantitatively assessed by the MTT assay.[41-42] HeLa and H9C2 cells were chosen as models for cancer and normal cells, respectively. The HeLa and H9C2 cells were incubated in a fetal bovine serum (FBS) free culture medium containing N-C-dots at different concentrations for 24 and 48 h, respectively. Figure 5 shows the viability of HeLa and H9C2 cells incubated with N-C-dots in a wide concentration range from 0 to 100 ug/mL, and no apparent cell loss was observed. The results suggested that the N-C-dots exhibit biologically low cytotoxicity for both HeLa and H9C2 cells and can be used for various bio-applications.

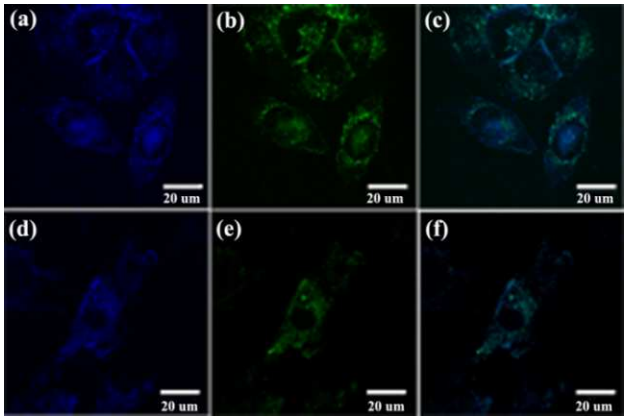

Figure 6. Confocal microscopy images of (a,b) HeLa and (d,e) H9C2 cells treated with N-C-dots (50 μg/mL) for 6 h and then irradiated under 405 and 488 nm, respectively; (c) Merged images of (a) and (b); and (f) Merged images of (d) and (e).

Based on their low toxicity, powerful fluorescence, and excellent resistance to photobleaching, the N-C-dots were directly used for cell imaging to demonstrate one of their promising applications. The HeLa and H9C2 cells were incubated with N-C-dots (50 μg/mL) for 6 h, and fluorescence images were recorded by confocal microscopy. Bright blue and green images were observed for HeLa cells incubated with N-C-dots upon light irradiation of 405 and 488 nm, respectively, caused by the strong fluorescence emitted by N-C-dots (Figures 6a and b). Surprisingly, the regions at both the cell wall and nucleus were bright, indicating that a large amount of C-dots has been internalized into the cells and even in the nucleus. When being merged into one picture, Figure 6a and b perfectly overlap (Figure 6c). A similar phenomenon was observed for H9C2 cells (Figures 6d-f). However, the nucleus region in H9C2 was dark, implying that the N-C-dots cannot enter the H9C2 nucleus, probably because of the denser nuclear membrane and smaller nuclear pores of H9C2. Therefore, N-C-dots can act as ideal fluorescent nanomaterials for various cell imaging applications.

Conclusions

In summary, we successfully developed a facile but effective method for the mass preparation of N-C-dots by the direct heating of the solid mixture of FA and SC. The N-doping content of the resulting N-C-dots can be easily and precisely tuned from 0% to 14% by adjusting the SC:FA mass ratio. Uniform C-dots and N-C-dots with some honeycomb-like order structures were obtained, with sizes ranging from 1 to 3 nm in diameter. The C-dots and N-C-dots emitted blue and green fluorescence based on the excitation wavelength and N-doping content. The nitrogen content affected not only the emission wavelength but also the emission quantum yield. This study provides a new method to achieve the mass production of N-C-dots with tunable emissions for various applications. Because of their low toxicity, powerful fluorescence, and high photostability, the N-C-dots can enter various cells and serve as ideal candidates for multicolour cell imaging.

Acknowledgements

This work was supported by the National Science Foundation of China (21174087, 21474079), the Program for New Century Excellent Talents in University (NCET-13-0453), the China Postdoctoral Science Foundation (2013M540738, 2014T70909), the Fundamental Funds for the Central Universities (08142027, 08143101).

Notes and references

[a] *School of Science; State Key Laboratory for Mechanical Behavior of Materials, Xi'an Jiaotong University, Xi'an, 710049, P. R. China.*
[b] *School of Chemistry and Chemical Technology; State Key Laboratory of Metal Matrix Composites, Shanghai Jiaotong University, Shanghai, 200240, P. R. China.*

[c] *School of Life Science and Technology, Xi'an Jiaotong University, Xi'an, 710049, P.R. China.*
[d] *International Center for Dielectric Research, Xi'an Jiaotong University, Xi'an, 710049, P.R. China.*

† Electronic Supplementary Information (ESI) available: FL spectra of C-dots at different concentration, FTIR spectra of N-C-dots prepared with different mass ratio of SC to FA, FL spectra of N-C-dots (0.5 mg/mL) prepared at different reaction time, FL spectra of C-dots and N-C-dots under irradiation of 490 nm, FL lifetime of the C-dots under irradiation of 365 nm, FL spectra of N-C-dots under 365 nm light (2 W) at different irradiation time, and XPS analysis of N-C-dots. See DOI: 10.1039/b000000x/

1 J. Peng, W. Gao, B. K. Gupta, Z.Liu, R. Romero-Aburto, L. H. Ge, L. Song, L. B.Alemany, X. B. Zhan, G. H. Gao, *Nano. Lett.* **2012,** *12* (2), 844

2 S. J. Zhu, J. H. Zhang, C. Y. Qiao, S. J. Tang, Y. F. Li, W. J. Yuan, B. Li, L. Tian, F. Liu, R. Hu, *Chem. Commun.* **2011,** *47* (24), 6858

3 S. Chen, X. Hai, C. Xia, X. W. Chen, J. H Wang, *Chem. Eur. J.* **2013,** *19* (47), 15918

4 M. Nurunnabi, Z. Khatun, K. M. Huh, S. Y. Park, D. Y. Lee; K. J. Cho, Y. K. Lee, *Acs Nano* **2013,** *7* (8), 6858

5 Y. B. Song, S. J. Zhu, B. Yang, *Rsc. Adv.* **2014,** *4* (52), 27184;

6 H. J. Sun, N. Gao, K. Dong, J. S. Ren, X. G. Qu, *Acs Nano* **2014,** *8* (6), 6202-6210.

7 M. A. Sk, A. Ananthanarayanan, L. Huang, K. H. Lim, P. Chen, *J. Mater. Chem.* **2014,** *2* (34), 6954

8 L. B. Tang, R. B. Ji, X. M. Li, K. S.Teng, S. P. Lau, *Part. Part. Syst. Char.* **2013,** *30* (6), 523

9 S. N. Baker, G. A. Baker, *Angew. Chem. Int. Ed.* **2010,** *49* (38), 6726

10 C. J. Liu.; P. Zhang, X. Y. Zhai, F. Tian, W. C. Li. J. H.Yang, Y. Liu, H. B. Wang, W. Wang, W. G. Liu., *Biomaterials* **2012,** *33* (13), 3604

11X. Y. Li, H. Q. Wang, Y. Shimizu, A. Pyatenko, K. Kawaguchi, N. Koshizaki, *Chem. Commun.* **2011,** *47* (3), 932

12 P. Sun, B. Zhou, Y.Lin, W. Wang, K. Fernando, P. Pathak, M. J. Meziani, B. A. Harruff, X. Wang, H. F. Wang, *J. Am. Chem. Soc.* **2006,** *128* (24), 7756

13 B. X. Zhang, H. Gao, X. L. Li, *New. J. Chem.* **2014,** *38* (9), 4615

14 M. H. Xu, G. L. He, Z. H. Li, F. J. He, F. Gao, Y. J. Su, L. Y. Zhang, Z. Yang, Y. F. Zhang, *Nanoscale* **2014,** *6* (17), 10307

15 L. B. Tang, R. B. Ji, X. M. Li, G. X. Bai, C. P. Liu, J. H. Hao, J. Y. Lin, H. X. Jiang, K. S. Teng, Z. B. Yang, *Acs Nano* **2014,** *8* (6), 6312

16 Z. Qian, .J Ma, X. Shan, H. Feng, L. Shao, J. Chen, *Chem. Eur. J.* **2014,** *20* (11), 2983

17 N.Y. Liu, J. Liu, W. Q. Kong, H. Li, H. Huang, Y. Liu, Z. H. Kang, *J. Mater. Chem. B* **2014,** *2* (35), 5768

18 Y. Li, Y. Zhao, H. H. Cheng, Y. Hu, G. Q. Shi, L. M. Dai, L. T. Qu, *J. Am. Chem. Soc* **2012,** *134* (1), 15

19 S. Dey, A. Govindaraj, K. Biswas, C. N. Rao, *Chem. Phys. Lett.* **2014,** *595*, 203

20 D. Qu, M. Zheng, P. Du, Y. Zhou, L. G. Zhang, D. Li, H. Q. Tan, Z. Zhao, Z. G. Xie, Z. C. Sun, *Nanoscale* **2013,** *5* (24), 12272

21 Z. T. Fan, Y. C. Li, X. H. Li, L. Z. Fan, S. X. Zhou, D. C. Fang, S. H. Yang, *Carbon* **2014,** *70*, 149

22 S. K Hamalainen, Z. X. Sun, M. P. Boneschanscher, A. Uppstu, M. Ijas, A. Harju, D. Vanmaekelbergh, P. Liljeroth, *Phys. Rev. Lett.* **2011,** *107* (23), 236803

23 L. L. Li, J. Ji. R. Fei; C. Z. Wang, L. Qian, J. R. Zhang, L. P. Jiang, J. J. Zhu, *Adv. Funct. Mater.* **2012,** *22* (14), 2971

24 Y. Li, Y. Hu, Y. Zhao, G. Q. Shi, L. E. Deng, Y. B. Hou, L. T. Qu, *Adv. Mater.* **2011,** *23* (6), 776

25 J. J. Liu, X. L. Zhang, Z. X. Cong, Z. T. Chen, H. H. Yang, G. N. Chen, *Nanoscale* **2013,** *5* (5), 1810

26 M. Zhang, L. L. bai, W. H. Wang, W. J. Xie, H. Ma, Y. Y. Fu, D. C. Fang, H. Sun, L. Z. Fan, M. Han, *J. Mater. Chem.* **2012,** *22* (15), 7461

27 Y. Q. Dong, H. C. Pang, H. B. Yang, C. X. Guo, J. W. Shao, Y. W. Chi, C. M. Li, T. Yu, *Angew. Chem. Int. Ed.* **2013,** *52* (30), 7800

28 X. Wu, W. X. Wang, J. Chen, M. Wu. J. X. Zhao, *J. Mater. Chem. C* **2013,** *1* (31), 4676

29 Y. Q. Dong, J. W. Shao, C. Q. Chen, H. Li, R. X. Wang, Y. W. Chi, X. M. Lin, G. N. Chen, *Carbon* **2012,** *50* (12), 4738

30 Z. Ma, H. Ming, H. Huang, Y. Liu, Z. H. Kang, *New. J. Chem.* **2012,** *36* (4), 861

31 S. Dey, P. Chithaiah, S. Belawadi, K. Biswas, C. N. Rao, *J. Mater. Res.* **2014,** *29* (3), 383

32 Y. Q. Zhang, D. K. MA, Y. Zhuang, X. Zhang, W. Chen, L. L. Hong, Q. X. Yan, K. Yu, S. M. Huang, *J. Mater. Chem.* **2012,** *22* (33), 16714

33 Q. Liu, B. D. Guo, Z. Y. Rao, B. H. Zhang, J. R. Gong, *Nano Lett.* **2013,** *13* (6), 2436

34 L. J. Meng, X. K. Zhang, q. H. Lu, Z. F. Fei, P. J. Dyson, *Biomaterials* **2012,** *33* (6), 1689

35 L. J. Meng, X. K. Zhang, Q. H. Lu, Z. F. Fei, P. J. Dyson, *Biomaterials* **2009,** *30* (30), 6041

36 Y. Q. Dai, H. Long, X. T. Wang, Y. M. Wang, Q. Gu, W. Jiang, Y. C. Wang, C. C. Li, T. H. Zeng, Y. M. Sun, *Part. Part. Syst. Char.* **2014,** *31* (5), 597

37 M. C. Hsiao, S. H. Liao, M. Y. Yen, P. I. Liu, N. W. Pu, C. A. Wang, C. C. Ma, *Acs Appl. Mater. Interf.* **2010,** *2* (11), 3092

38 D. Qu, M. Zheng, L. G. Zhang, H. F. Zhao, Z. G. Xie, X. B. Jing, R. E. Haddad, H. Y. Fan, Z. C. Sun, *Sci. Rep.* **2014,** *4*.5294

39 S. J. Zhu, L. Wang, B. Li, Y. B. Song, X. H. Zhao, G. Y. Zhang, S. T. Zhang, S. Lu, J. H. Zhang, H. Y. Wang, *Carbon* **2014,** *77*, 462

40 S. J. Zhu, J. H. Zhang, S. J. Tang, C. Y. Qiao, L. Wang, H. Y. Wang, X. Liu, B. Li, Y. F. Li, W. L. Yu, *Adv. Funct. Mater.* **2012,** *22* (22), 4732

41 P. Nigam, S. Waghmode, M. Louis, S. Wangnoo, P. Chavan, D. Sarkar, *J. Mater. Chem. B* **2014,** *2* (21), 3190

42 Z. H. Wang, J. F. Xia, C. F. Zhou, B. Via, Y. Z. Xia, F. F. Zhang, Y. H. Li, L. H. Xia, J. Tang, *Colloids Surf. B Biointerf.* **2013,** *112*, 192

Table of contents entry

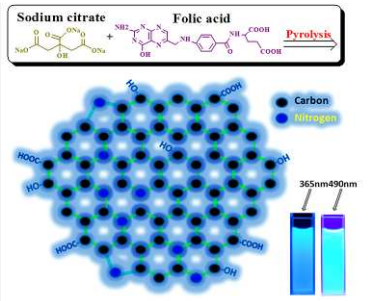

A facile but effective bottom-up method was developed for the mass preparation of N-doped carbon dots (N-C-dots) for cell imaging.